

# Effects of salts and temperature on rheological and viscoelastic behavior of low molecular weight HPAM solutions

Fabián Andrés Tapias Hernandez\*; Juan Carlos Lizcano Niño; Rosângela Barros Zanoni Lopes Moreno.

School of Mechanical Engineering, University of Campinas. Campinas, São Paulo, Brazil

\*E-mail: fabian.tapias@hotmail.com

## Abstract

The hydrolyzed polyacrylamide (HPAM) is the most often used polymer in Enhanced Oil Recovery (EOR) activities. The molecular weight of HPAM has a direct relationship with the molecular size and the permeability of the porous media through the polymer will be injected. The polymer flooding has been documented in EOR process for different types of geologic formations, salinity and temperature conditions. This work aims to investigate the effects of salts and temperature on the rheological and viscoelastic behavior of polymer solutions for low permeability formations. The knowledge of the rheological behavior is imperative to evaluate the mobility ratio improvement, while elastic properties are associated with an additional oil mobilization. For this reason, an experimental study was conducted using Flopaam 3230S over two temperatures and three different brine compositions. The flow curves show a significant reduction polymer viscosity when the concentration of ionic species increases, reducing the hydrodynamic size of the polymer. The Ostwald-de Waele law and Carreau-Yasuda model were used to describe the rheological properties of the solutions. The variation of viscosity with temperature was also studied and adjusted to Arrhenius equation. Regarding the viscoelastic properties, comparisons were made between the different polymeric solutions, and we observed the reduction of the linear viscoelastic region (LVR) according to the increase of temperature, divalent ions concentration, and more diluted solutions. The viscous modulus is predominant for all solutions. These results contribute to the design of low molecular weight polymeric solutions under conditions of salinity with a high concentration of divalent ions, which is useful for low permeability formations.

**Keywords:** Polymeric Solutions, Rheological Behavior, Viscoelastic Behavior, Low Molecular Weight HPAM, Enhanced Oil Recovery.

## Efectos de sales y temperatura en el comportamiento reológico y viscoelástico de soluciones de HPAM de bajo peso molecular

### Resumen

La poliacrilamida parcialmente hidrolizada (HPAM) es el polímero sintético más usado en actividades de recuperación mejorada de petróleo (EOR). El peso molecular del HPAM tiene una relación directa con el tamaño molecular y la permeabilidad del medio poroso a través del cual será inyectado el polímero. La inyección de polímero ha sido reportada en procesos EOR en diferentes formaciones geológicas, salinidades y temperatura. Este trabajo foca en investigar los efectos de diferentes sales y la temperatura sobre el comportamiento reológico y viscoelástico de soluciones poliméricas para formaciones de baja permeabilidad. Conocer el comportamiento reológico es de vital importancia para evaluar la mejora de la razón de movilidad de los fluidos, mientras que las propiedades elásticas están asociadas con una adicional movilización de petróleo. Por estas razones, se desarrolló un estudio experimental usando Flopaam 3230S bajo dos temperaturas y tres composiciones de salmuera diferentes. Las curvas de flujo muestran una reducción significativa de la viscosidad con el aumento de la concentración de especies iónicas, reduciendo el tamaño hidrodinámico del polímero. La ley de Ostwald-de Waele y el modelo de Carreau-Yasuda fueron usados para describir las propiedades reológicas de las soluciones. La variación de viscosidad respecto a la temperatura fue estudiada y ajustada según la ecuación de Arrhenius. Respecto a las propiedades viscoelásticas, comparando las diferentes soluciones poliméricas fue observada la reducción de la región viscoelástica lineal (LVR) a medida que se incrementa la temperatura y la concentración de iones divalentes, así como cuando las soluciones son más diluidas. El modulo viscoso es predominante para todas las soluciones. Estos resultados contribuyen al diseño de soluciones poliméricas de bajo peso molecular útiles para formaciones de baja permeabilidad en condiciones de salinidad con alto contenido de iones divalentes.

**Palabras claves:** Soluciones poliméricas, comportamiento reológico, comportamiento viscoelástico, HPAM de bajo peso molecular, recuperación mejorada de petróleo.

**Cita:** Tapias, F.A., Lizcano, J.C. & Lopes, R. B. (2018). Effects of salts and temperature on rheological and viscoelastic behavior of low molecular weight HPAM solutions. *Revista Fuentes: El reventón energético*, 16(1), 19-35.



## Introduction

Mobility control is one of the most important concepts in any enhanced oil recovery process (Sheng, 2011). It can be achieved through injection of chemicals to change displacing fluid viscosity, with the addition of foams to reduce specific fluid relative permeability or through injection of chemicals to modify the wettability (Abidin, Puspasari & Nugroho, 2012).

Those procedures are known as Chemical methods for Enhanced Oil Recovery (CEOR) (Lake, 1991). The polymer flooding is one of these methods and is used to change displacing fluid mobility by adding water-soluble polymers. A better mobility control improves the vertical and areal sweep efficiencies (Melo et al., 2002) and also lowers the total volume of water needed to achieve the residual oil saturation (Martin, García, Lizcano & Buendia, 2014). Additionally, polymer adsorption decreases the permeability to water, also reducing the mobility (Littmann, 1988)(Needham, Co & Doe 1987). Two kinds of polymers are potentially used in EOR process, the synthetic polymers like HPAM and the biopolymers like Xanthan gum (XG) (Sorbie, 2013)(Green & Willhite, 1998) (Molano, Navarro & Díaz, 2014). HPAM polymers are much more widely used than XG because it has advantages in price and large-scale production (Sheng, 2013). Besides that, HPAM solutions are more viscoelastic than XG solutions. The term Partially Hydrolyzed is associated with the conversion of some amide groups ( $CONH_2$ ) to carboxyl groups ( $COO^-$ ) of the Polyacrylamide. This process is known as Hydrolysis and ranges from 15% to 35% in commercial products (Wang, Han, Shao, Hou & Seright, 2008). In other words, the HPAM is a flexible polyelectrolyte with negative charges on the carboxylate groups, which implies a strong interaction between the polymer chains and any cation present in the water (Lopes, Silverira & Moreno., 2014).

When a monovalent salt (i.e., NaCl, KCl) is added in a homogenous HPAM solution, the carboxylic group is surrounded by the cations, which shield the charge and reduce the carboxylic group repulsion, the hydrodynamic volume becomes smaller, therefore, the viscosity decreases (Sheng, 2011). When divalent salts are present (i.e.,  $MgCl_2 \cdot 6H_2O$ ,  $CaCl_2 \cdot 2H_2O$ ) in an HPAM solution, their effect is complex (Zhu, Wei, Wang, & Feng, 2014)(Reichenbach-Klinke, Langlotz, Wenzke, Spindler, Brodt, 2011). Due to their higher positive charges, divalent ions are more effective in shielding negative charges on the polymer chain than the monovalent ions. Consequently, the polymer coils

up at lower divalent ions concentration and reduces the hydraulic radius of the polymer chain, which causes the degree of polymer chain entanglement to diminish (Bataweel & Nasr-El-Din, 2012; Levitt & Pope, 2008).

Dissolved salts in a solution of a flexible polyelectrolyte cause mutual repulsion of the charges along the chain (Martin & Páez, 2017). This effect is represented by the ionic strength ( $I_s$ ) of the solution (Sorbie, 2013).

$$I_s = \frac{1}{2} \sum m_i z_i^2 \quad (1)$$

where  $m_i$  is the molar concentration of the  $i$ th ion and  $z_i$  is its charge.

The temperature also influences the rheological behavior of the polymeric solution generating a detrimental effect on the viscosity, significant changes are reported for 333,15 and 363,15 K (Muller, 1981). Several authors (Ghosh & Maiti, 1997; Maiti and Mahapatro, 1988; Zhou, Willett & Carriere, 2000) documented that the relationship between the apparent viscosity of polymeric solution and temperature satisfies the Arrhenius equation:

$$\eta = A \exp\left(\frac{\Delta E_\eta}{RT}\right) \quad (2)$$

where  $\eta$  is the apparent viscosity of the polymeric solution (Pa\*s),  $A$  is a constant characteristic of polymeric solution (Pa\*s),  $T$  is the absolute temperature (K),  $\Delta E_\eta$  is the viscous activation energy or the activation energy for flow (kJ/mol), and  $R$  is the universal gas constant ( $kJ \cdot K^{-1} \cdot mol^{-1}$ ).

A plot of  $\ln(\eta)$  vs  $1/T$  gives a straight line with a slope of  $\Delta E_\eta/R$ . The viscous activation energy is related to the dependence of the viscosity on temperature of the polymeric solution, and higher viscous activation energy indicates greater influence of the temperature on the viscosity (Samanta, Bera, Ojha & Mandal, 2010) alkali, and surfactants on the rheological properties of partially hydrolyzed polyacrylamide (PHPAM).

The polymers are classified as pseudoplastic fluids under the majority of the conditions (Castro-García, et al, 2016). These types of fluids show a reduction of the viscosity as shear rate increases (Díaz, Navarro & Tavera, 2007). They are known as shear thinning fluids (Barnes, Hutton & Walters, 1989) and are represented by a curve with three notable regions. The first region is a plateau characterized by a constant viscosity at very low shear rates or stress ( $\eta_0$ ). The second region describes

the shear thinning behavior, known as a pseudoplastic region. The third region is also a plateau and indicates the final of the pseudoplastic region and the beginning of the constant behavior of viscosity for high rates ( $\eta_\infty$ ).

There are several models to describe the form of that curve (Sorbie, 2013), but the most commonly used is the power law model, also called as Ostwald-de Waele law (Cardenas, López y Pinto, 2011; Sheng, 2011), which describes the pseudoplastic region. Mathematically, the formula is:

$$\tau = K\dot{\gamma}^n \quad (3)$$

where  $\tau$  is the shear stress (Pa),  $\dot{\gamma}$  is the shear rate ( $s^{-1}$ ),  $n$  is the flow behavior index (dimensionless), and  $K$  is the consistency index ( $Pa \cdot s^n$ ). For pseudoplastic fluids,  $n < 1$ . The equation describes with a good accuracy only the pseudoplastic regime, however it is inaccurate at high and low shear rates (Perttamo, 2013).

A more satisfactory model for the complete shear rate range, capable of fitting data in the three regions of the characteristic curves of thinning fluids, is the Carreau-Yasuda model (Sheng, 2011; Yasuda, Armstrong & Cohen, 1981).

$$\tau = \gamma \left( \eta_\infty + \frac{\eta_0 - \eta_\infty}{(1 + (\lambda\dot{\gamma})^a)^{\frac{1-n}{a}}} \right) \quad (4)$$

where ( $\eta_\infty$ ) is the limiting viscosity at the upper shear rate and is generally taken as water viscosity (Sheng, 2011),  $n$  is the same as power law index,  $\lambda$  is a time constant generally taken as 2 (Sheng, 2011),  $\eta_0$  is the viscosity at very low shear rates or stress.

If the viscosity versus polymer concentration is plotted for a particular shear rate, the dilute and semidilute regimes are identified. In the first, the macromolecules are separated from each other and behave independently. In the semi-dilute regime, the macromolecules are entangled and thus impose frictions on each other, increasing the viscosity of the fluid. The overlapping concentration  $C^*$  measures the transition between these regimes and is characterized by a change in the shape of the viscosity concentration plot (Al Hashmi et al., 2013; Sorbie, 2013). Concentration values below  $C^*$  are associated with diluted regime and values above  $C^*$  with the semidilute regime.

There is another important property that needs to be considered during the design for polymer flood

operations. It is the viscoelasticity (Ordoñez & Fajardo, 2015). Laboratory results have reported an increase in oil recovery when are using viscoelastic polymeric solutions (Huifen, Fanshun, & Junzheng, 2004; Wang et al., 2001). This improvement has been attributed to the elastic properties of the polymeric solutions, and their effect on the displacement efficiency increase (Jiang et al., 2008; Urbissinova, Trivedi, & Kuru 2010; Wang, Wang, Wu, Xia, & Yin, 2007). This study is focused on analyzing the behavior of the storage modulus ( $G'$ ), also named elastic modulus, which is related to the Hooke's law (Sorbie, 2013). It is associated with "memory" or elasticity of the polymeric solution, it means, the material returns to its original configuration when any deforming force is removed. Moreover, the changes caused on the loss modulus ( $G''$ ), known as viscous modulus (Barnes et al., 1989), gives information about the viscous properties of the solution. If  $G'$  and  $G''$  exist simultaneously and are parallel horizontally in an amplitude sweep test (AST), we can affirm that the material has a linear viscoelastic region (LVR) (Silveira, Lopes, & Moreno 2016; Sorbie, 2013).

During a polymer flooding, a previous rheological laboratory study allows designing the better polymeric solution under a target composition and conditions, aiming to minimize the rheological changes within the reservoir. For this reason, this study is focused on evaluating the rheological behavior and some viscoelastic properties on three different polymeric solutions. These solutions were prepared using Flopaam 3230S, and synthetic brines (SB) including monovalent and divalent salts and different ionic strengths. The tests were made at two temperatures. The rheological behavior of the polymeric solutions was adjusted using the power law and the Carreau-Yasuda model. Finally, the temperature effects on the viscosity were modeled using the Arrhenius equation.

## Experimental section

### Materials

A Synthetic HPAM (Flopaam 3230S, SNF Floerger) was selected to run the tests. This polymer has a molecular weight (Mw) of  $5 \times 10^6$  g/mol, 30% of hydrolysis degree, water content less than 1% and thermal stability up to 433,15 K (Melo & Lucas, 2008).

Table 1 shows the synthetic brines used. Mainly, the table includes the type of salt and their respective concentration and ionic strength.

**Table 1.** Synthetic Brine (SB) Composition

Salt	Mw [g/mol]	Brine I		Brine II		Brine III	
		Concentration [g/L]	Ionic Strength [mol/L]	Concentration [g/L]	Ionic Strength [mol/L]	Concentration [g/L]	Ionic Strength [mol/L]
NaCl	58.44	5.4932	0.0940	7.0937	0.1214	6.000	0.1027
KCl	74.55	0.1496	0.0020	-	-	-	-
CaCl <sub>2</sub> ·2H <sub>2</sub> O	147.02	1.6647	0.0340	-	-	-	-
MgCl <sub>2</sub> ·6H <sub>2</sub> O	203.3	0.4951	0.0073	-	-	-	-
NaHCO <sub>3</sub>	84.007	-	-	-	-	1.0937	0.0130
<b>TOTAL</b>		7.8026	0.1373	7.0937	0.1214	7.0937	0.1157

### Preparation of HPAM Solutions

The procedure followed was API RP 63. A stock HPAM solution containing 5000 ppm of the polymer was prepared using the synthetic brines mentioned in Table 1. Every SB was deaerated using a vacuum bomb. These HPAM solutions were agitated using a magnetic stirrer during (5 – 7) h to form a consistent solution, i.e., the solution exhibited a homogenous aspect, and it did not have insoluble particle (fisheye). All of the HPAM solutions were prepared carefully with the minimum degree of agitation (60-80 rpm) to avoid mechanical degradation of the long-chain molecules. The stock solutions were left still overnight to ensure full hydration.

Then, the stock solutions were diluted with SB up to 100 ppm. The new solutions were put into a beaker and homogenized by magnetic stirrer at low speed (80 rpm) for 10 minutes. All of the HPAM solutions were stored in closed recipients to minimize oxygen uptake.

### Measurements

In the present study, the rheological and viscoelastic parameters were measured using a rheometer HAAKE MARS III, which is a high precision instrument. The sensor used was the concentric cylindrical (DG41) due to this is preferable for low viscous fluids. The temperature control used was the THERMO HAAKE C25P refrigerated bath with a Phoenix II Controller. A new sample was applied for each test, and every data analyzed were within the measuring range of the sensor and were compared with the rheological behavior of a fluid pattern (IPT-83).

The flow curves are recorded at shear rates between ( $10^{-1}$  and  $10^3$ )  $s^{-1}$  with 20 measurement points. These flow curves were used for the analysis of viscosity, shear stress, and temperature effect. The overlap

concentration is determined at the shear rates of interest. Flow curves reveal information about the ability of the polymer to flow under different shear rate and target process conditions (Samanta et al., 2010).

The viscoelastic behavior was determined with frequency sweep tests (FST) covering a range of 0.062832 – 628.32 Rad/s with 25 measurements points. For this study, it was necessary to choose shear stress within the LVR of amplitude sweep tests (AST) conducted between 0.001 – 100 Pa, with 30 measurements points. These measurements were carried out for at least two times at two temperatures 298.15 and 323.15 K to ensure the repeatability of the results.

## Results and discussion

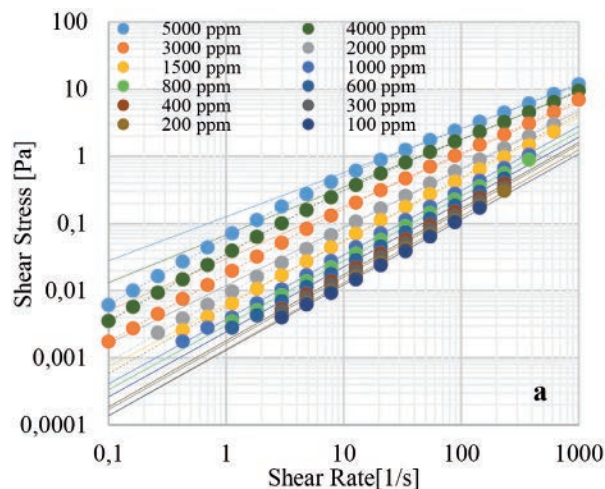
### Shear Stress and Shear Rate Curves

This section shows the results for shear stress-shear rate data of the prepared HPAM solutions with different polymer salt concentration obtained at two temperature levels. The solutions with high polymer concentration present the first plateau and the pseudoplastic behavior. In these cases, both regions can be fit using the Carreau-Yasuda model. Adjusted curves showed good accuracy ( $R^2$  values showed in Appendix A is closer to 1).

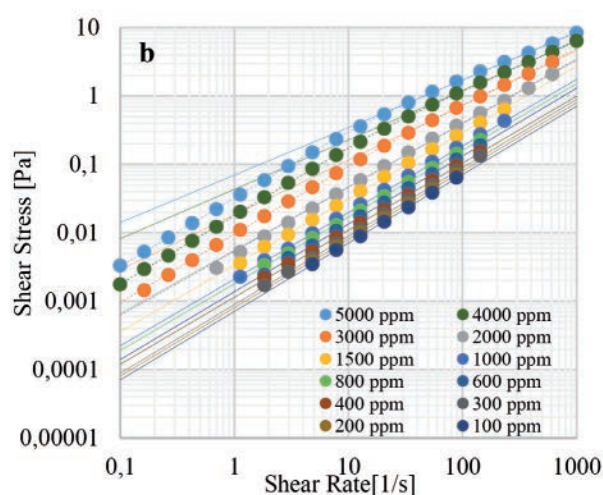
Whereas for low polymer concentration, the Carreau-Yasuda model became similar to Ostwald-de Waele law, it happens when the value of  $\eta_a$  becomes approached to the value of  $\eta_0$ . In this case, the calculation to obtain the Carreau-Yasuda constants carries a greater uncertainty, i.e., the  $R^2$  get away from 1.

Figure 1a,b shows the fits obtained for HPAM Solution with Brine I at 298.15 and 323.15 K. For Carreau-Yasuda model was used  $\eta_a$  as 0.93 and 0.6 for each temperature.

These values are the SB viscosity at these temperatures. Dashed lines represent the Carreau-Yasuda fits, and continuous lines represent the Ostwald de Waele fits.



The parameters for the best fits using the mentioned models for all HPAM solutions are presented in Appendix A.



**Figure 1a, b.** Shear Stress vs. Shear Rate for HPAM Solution with Synthetic Brine I and different polymer concentrations at **a** 298.15 K; **b** 323.15 K. **Dashed lines** - Carreau-Yasuda fits, **continuous lines** - Ostwald-de Waele fits.

By eq 3, the values of  $K$  and  $n$  can be calculated from the intercept and slope of the best fitted straight line, respectively in the Figure 1a,b (see continuous lines). All of samples showed good fits to the theoretical models ( $R^2 > 0.98$ ), and showed that when more diluted was the solution is closer to the Newtonian fluid behavior ( $n = 1$ ), presenting negligible changes with shear rate.

As the polymer concentration increases, the consistent index decrease. That is to say, as the solution has a high polymer concentration it also has greater resistance to the fluid flows. Therefore, at a fixed shear rate the solution exhibits larger shear stress, as presented by other authors (Lopes et al., 2014; Maiti & Mahapatro, 1988; Silveira et al., 2016)(Maiti & Mahapatro, 1988; Silveira et al., 2016). It is related to the raising in the intermolecular entanglement. (Bataweel & Nasr-El-Din, 2012; Sorbie, 2013)

The viscosity curves for SB solutions of HPAM at different shear rates and concentrations are shown in Figures 2-4. The viscosity of the solutions decreased with decreasing of polymer concentration and therefore have low shear stress, as expected. Besides that, when shear rate increases, the solution viscosity decrease, elucidating that the HPAM solutions exhibit shear thinning behavior as was mentioned by other authors (Barnes et al., 1989; Samanta et al., 2010). This behavior

is due to uncoiling and aligning of the polymer chains upon exposure to shear flow.

In Figures 2-4, the viscosities show a plateau at low shear rates, it is  $\eta_0$ , which can be measured by extrapolating the viscosity curve to the viscosity at very low shear rate. Also, can be observed as the concentration decreases, the viscosity tends to lose the pseudoplastic region, and the plateau increases. This behavior turns the use of the Carreau-Yasuda model for low concentration unnecessary, since the Ostwald de Waele law gives a simpler and accurate method to calculate the viscosity behavior for these conditions. Comparing the series *a* and *b* from Figures 2-4, we also can see that temperature imposes a detrimental effect on the HPAM solutions viscosity.

### Temperature Effect on HPAM Solutions Viscosity

The viscosity of evaluated HPAM solutions presents a detrimental effect when the temperature increases, generating an increment in the average speed of the molecules within the liquid, thereby, the interaction time with neighboring polymer molecules decrease. As well as the temperature increases, the average intermolecular forces decrease. Similar behavior has been reported (Samanta et al., 2010; Silveira et al., 2016).

The Arrhenius equation (eq. 4) is used to correlating the effect of temperature on the viscosity of HPAM solutions. For this, a shear rate of  $7.8 \text{ s}^{-1}$  was selected,

which is approximated to the shear rate applied to the fluid in the reservoir (Melo et al., 2005; Melo & Lucas, 2008).

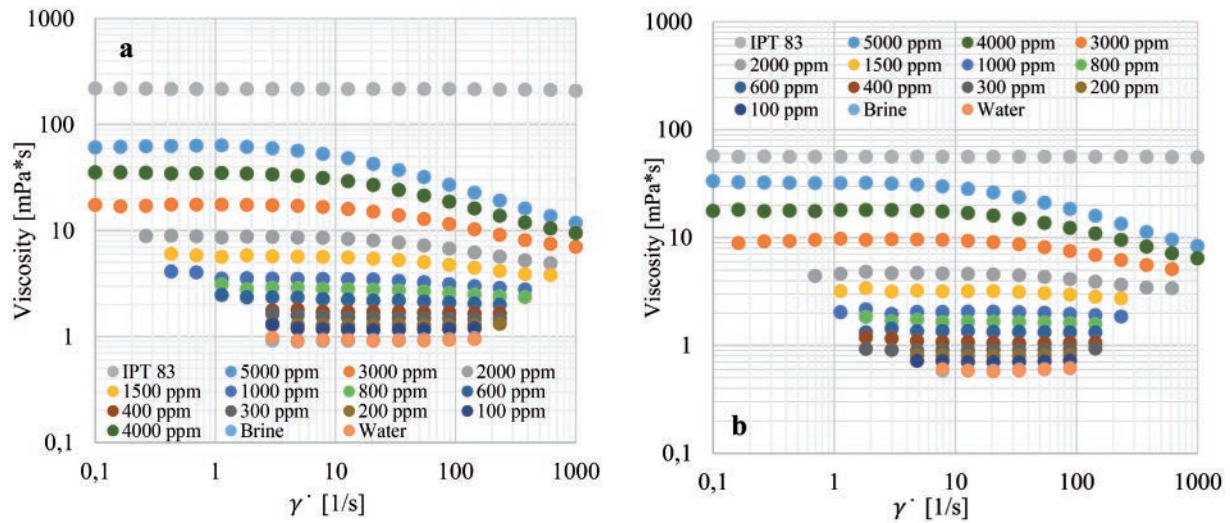


Figure 2a, b. Viscosity vs. Shear Rate for HPAM Solution with Synthetic Brine I and different polymer concentrations at a 298.15 K; b 323.15 K.

Appendix B shows the fit parameters for all HPAM solutions. We can see that the change in the  $\Delta E_\eta$  value is not meaningful regardless of the change on HPAM solution concentration. This result means that the viscous activation energy is almost independent of

the polymer concentration, corresponding to similar behaviors reported (Ghosh & Maiti, 1997; Maiti & Mahapatro, 1988). Otherwise, the  $\Delta E_\eta$  value is related to the influence of temperature on the viscosity of the HPAM solutions (Samanta et al., 2010).

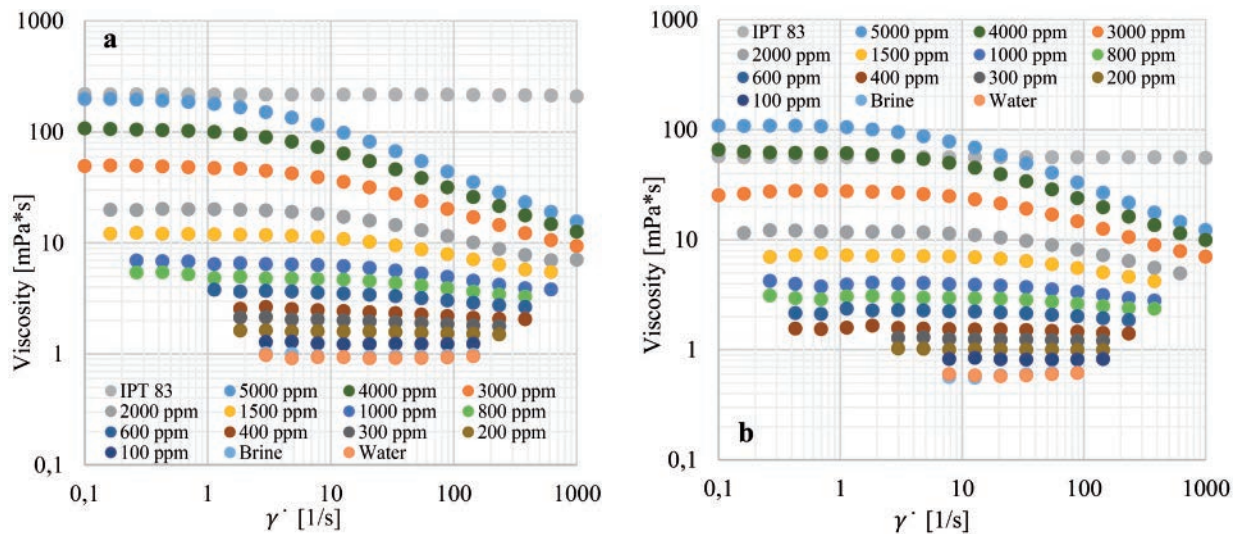
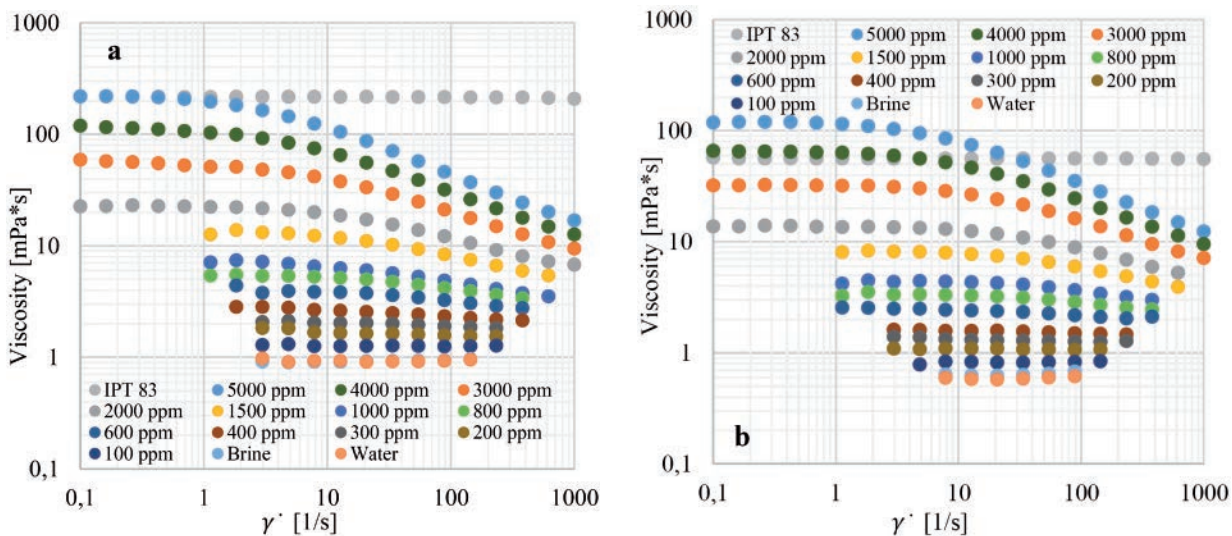
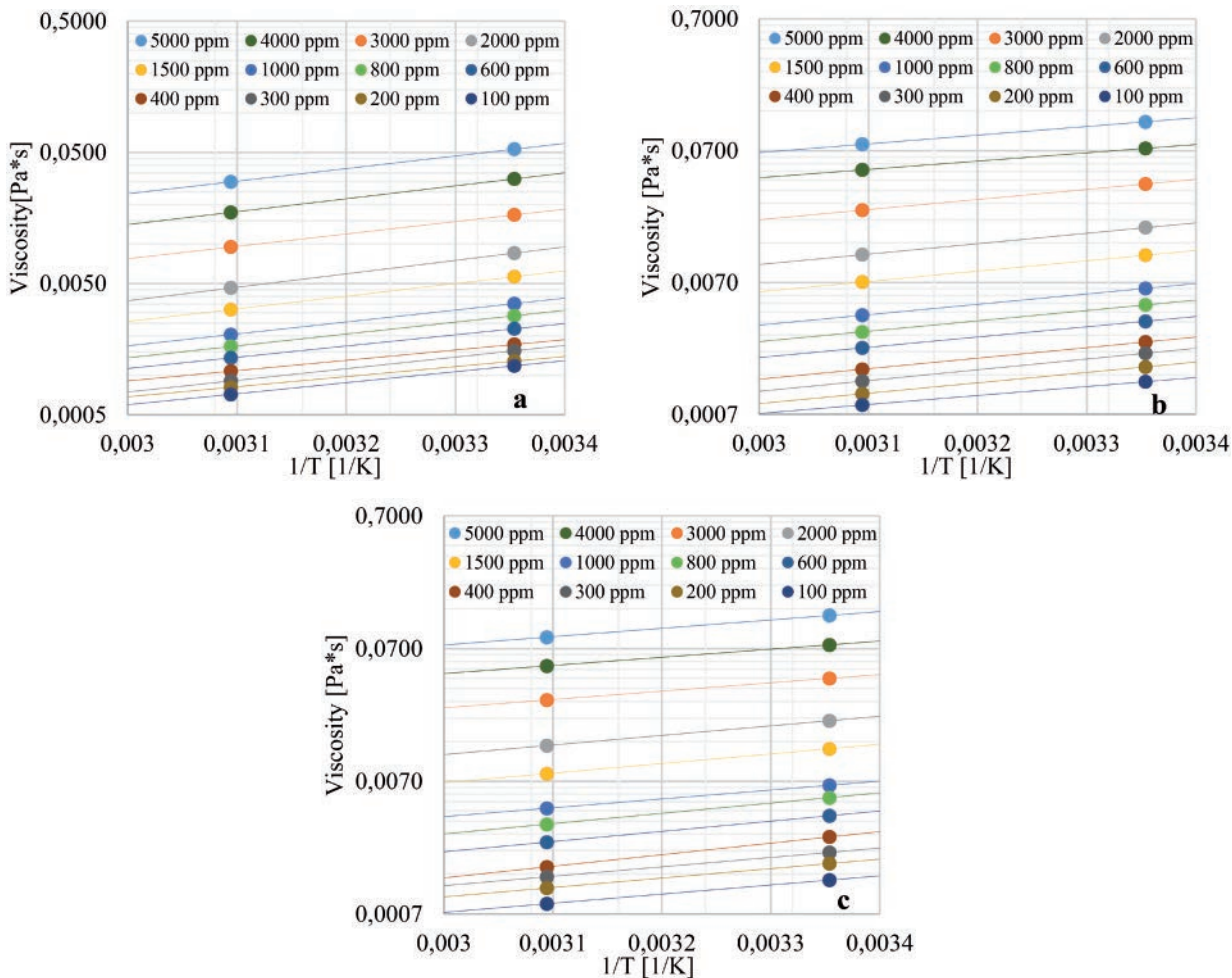


Figure 3a, b. Viscosity vs. Shear Rate for Polymer Solution with Synthetic Brine II and different polymer concentrations at a 298.15 K; b 323.15 K.



**Figure 4a, b.** Viscosity vs. Shear Rate for Polymer Solution with Synthetic Brine III and different polymer concentrations at a 298.15 K; b 323.15 K.



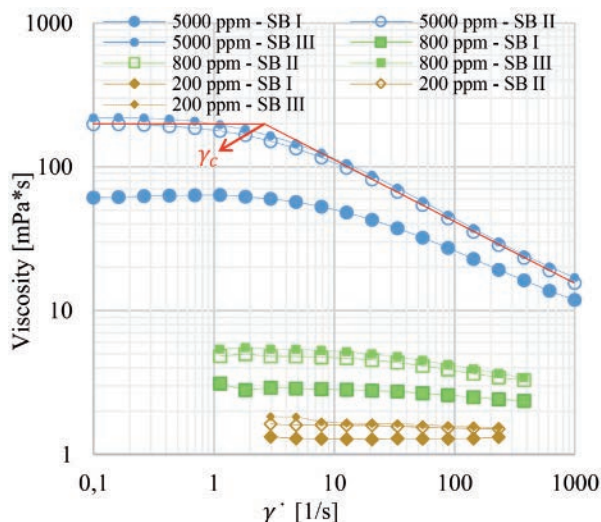
**Figure 5a-c.** Arrhenius plot of viscosity at a different concentration with shear constant  $\gamma=7.8s^{-1}$ , a HPAM Solution with SB I; b HPAM with SB II; c HPAM with SB III.

Fig. 5a-c show the reduction of the viscosity as a function of temperature for the HPAM solutions. We can observe that the HPAM solution prepared with SB I has the highest ionic strength. Moreover, divalent ions have the most significant effect on the viscosity reduction. Despite the difference in the ionic strength presented by the HPAM solutions prepared with SB II and SB III, the viscosity reduction as a function of temperature was not meaningful in both cases. The smallest viscosity reduction is exhibited by the HPAM solution prepared using SB III, which has the lowest ionic strength.

Notwithstanding, the viscosity reduction can slightly influence the displacement flooding efficiency at field operation, the largest contribution to the notable viscosity decreases is due to the presence of ions (monovalent and divalent ions) in the synthetic brine, which interacts with the polymer negative charges, neutralizing the effect of the macromolecular expansion.

### Salt's Effect on HPAM Solutions Viscosity

As was mentioned above, the existence of ions influences the rheological behavior strongly. As the concentration of the monovalent ions of  $\text{Na}^+$  increases, the apparent HPAM solution viscosity diminishes, particularly at the low shear rates (see Figure 6).



**Figure 6.** Viscosity vs. Shear Rate for HPAM with different SB composition and three different polymer concentrations (SB I:  $\text{Na}^+$ ,  $\text{Cl}^-$ ,  $\text{K}^+$ ,  $\text{Ca}^{+2}$ ,  $\text{Mg}^{+2}$ ; SB II: only  $\text{Na}^+$ ,  $\text{Cl}^-$ ; SB III:  $\text{Na}^+$ ,  $\text{Cl}^-$  and  $\text{HCO}_3^-$ ), at 298.15 K.

The same effect occurs at 323.15 K. The presence of  $\text{Na}^+$  generates shrinkage on the molecular chains. The effective neutralization of negative charges promotes a compression of the flexible chains. As the  $\text{Na}^+$  content

increases, the ionic strength due to electrostatic repulsion among the anions is shielded, while the double electrical layers on the polymer molecular chains are compressed. Other authors have presented a similar performance (Samanta et al., 2010; Sheng, 2011; Sorbie, 2013).

A critical shear rate represents the transition between the Newtonian behavior or initial plateau and the beginning of the shear-thinning behavior  $\gamma_c$  (see Figure 6). The reduction in the polymer chain size due to charge shielding according to the increase in  $\text{Na}^+$  concentration gives a higher critical shear rate. Accordingly, the Newtonian behavior will extend over a wider range of shear rate.

The reaction mechanism for monovalent cations ( $\text{Na}^+$ ,  $\text{K}^+$ ) can be summarized as an electrolyte charge-shielding effect, which results in molecule chains shrinking, thus, raising the flexibility and diminishing the hydrodynamic radius. On the other hand, there is a molecular process more complex such as the reaction of divalent cations ( $\text{Ca}^{2+}$ ,  $\text{Mg}^{2+}$ ). In this case, the polymer coils up at lower divalent ions concentration and reduces the hydrodynamic radius of the polymer chain, causing a reduction in the degree of polymer chain entanglement. Thus, they generated a more pronounced detrimental to the rheological behavior (Melo et al., 2002; Melo & Lucas, 2008).

### Overlapping concentration ( $C^*$ )

The effect on the  $C^*$  was analyzed for the three HPAM solutions. Figure 7a shows the behavior of these regimes and the  $C^*$  for shear rates of 7.8 and 143.8  $\text{s}^{-1}$  at 298.15 K. Figure 7b shows the  $C^*$  behavior at a shear rate of 7.8  $\text{s}^{-1}$  and both temperatures. In the Figures 7a-b, dashed lines and continuous lines represent the dilute and semidilute regimes, respectively.

In the figure 7a, we can observe that the  $C^*$  is an inverse function of the shear rate for the tested HPAM solutions, i.e., as the shear rate increases the  $C^*$  diminishes. Accordingly, as the macromolecules are closer from each other, the diluted regime decreases while the semidiluted increases. Furthermore, as expected, the apparent viscosity decreases while the shear rate increases and ions concentration increases. A similar performance was reported (Al Hashmi et al., 2013; Silveira et al., 2016).

That results are an indication of the detrimental effect generated by the monovalent and divalent ions on the rheological behavior of HPAM solutions.

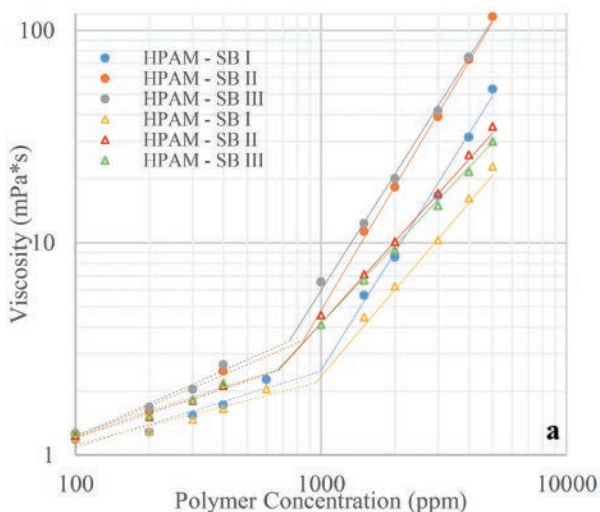


**Figure 7a.** Viscosity vs. Polymer concentration for different Brine compositions at 298.15 K. Where the **Circles** are  $\gamma=7.8s^{-1}$  and **triangles** are  $\gamma=143s^{-1}$ .

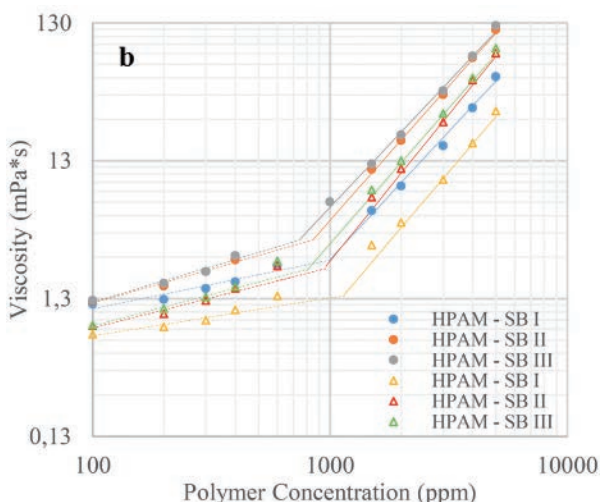


**Figure 7b** Viscosity vs. Polymer concentration for different Brine compositions at  $\gamma=7.8s^{-1}$ . Where the **Circles** are  $T=298.15$  K and **triangles** are  $T=323.15$  K.

The  $C^*$  behavior was mathematically adjusted by potential trend lines as it was made for others authors (Lopes et al., 2014; Silveira et al., 2016). Appendix C shows the fitting parameters.

Using the Figure 7b and the tables a-c of Appendix C to analyze the temperature effect, it is possible to see that the  $C^*$  is a direct function of the temperature. As higher is the temperature, lower are the average intermolecular forces (Samanta et al., 2010)alkali, and surfactants on the rheological properties of partially hydrolyzed polyacrylamide (PHPAM, whereby, the macromolecules are more separated and present a more free performance, an extended dilute regime, and higher

$C^*$  is obtained. Besides that, the apparent viscosity decreases while the temperature increases.

## Viscoelastic Behavior of HPAM Solutions

The increase in the oil recovery using viscoelastic HPAM solutions is due to the phenomena of expansion and contraction of the fluid during the flow through porous media (Urbissinova et al., 2010). This effect modifies the forces (capillary and viscous) that maintain the oil trapped and induces the movement of a part of the residual oil (Wang et al., 2001). Initially, we carried out AST for all HPAM solutions. The Figure 8a shows a comparison of results of AST for HPAM solutions with SB I and SB II. The figure 8b shows the same results for HPAM with SB II and SB III.

Then, was selected a shear stress range of 0.1 [Pa] to execute the FST. It shear stress was chosen to eliminate the risk of the test samples being oscillated outside LVR. The results at 0.1 [Pa] are shown in Figures 12a,b.

The linear viscoelastic region will be present between the ranges of shear rates where exists a plateau for a constant angular frequency for both  $G'$  and  $G''$ . The end of this plateau is named yield point, which represents the highest shear stress applied at a given condition before the network of associating polymers starts to deform and split up (Perttamo, 2013). The yield point is estimated at the end of the linear viscoelastic range on the dominating modulus. The Tables 2 and 3 show all yield points.

**Table 2.** Yield Point at 298.15 K for all HPAM solutions.

Polymeric Solution	Polymer Concentration	Yield Point @ 298.15 K	
		Shear Stress[Pa]	$G''$ [Pa]
HPAM+SB I	5000	0.3	0.3
	4000	0.1	0.19
HPAM+SB II	5000	0.3	0.58
	4000	0.2	0.37
HPAM+SB III	3000	0.1	0.21
	5000	0.3	0.59
HPAM+SB III	4000	0.2	0.38
	3000	0.1	0.22

**Table 3.** Yield Point at 323.15 K for all HPAM solutions.

Polymeric Solution	Polymer Concentration	Yield Point @ 323.15 K	
		Shear Stress[Pa]	$G''$ [Pa]
HPAM+SB II	5000	0.2	0.43
	4000	0.1	0.26
HPAM+SB III	5000	0.2	0.44
	4000	0.1	0.27

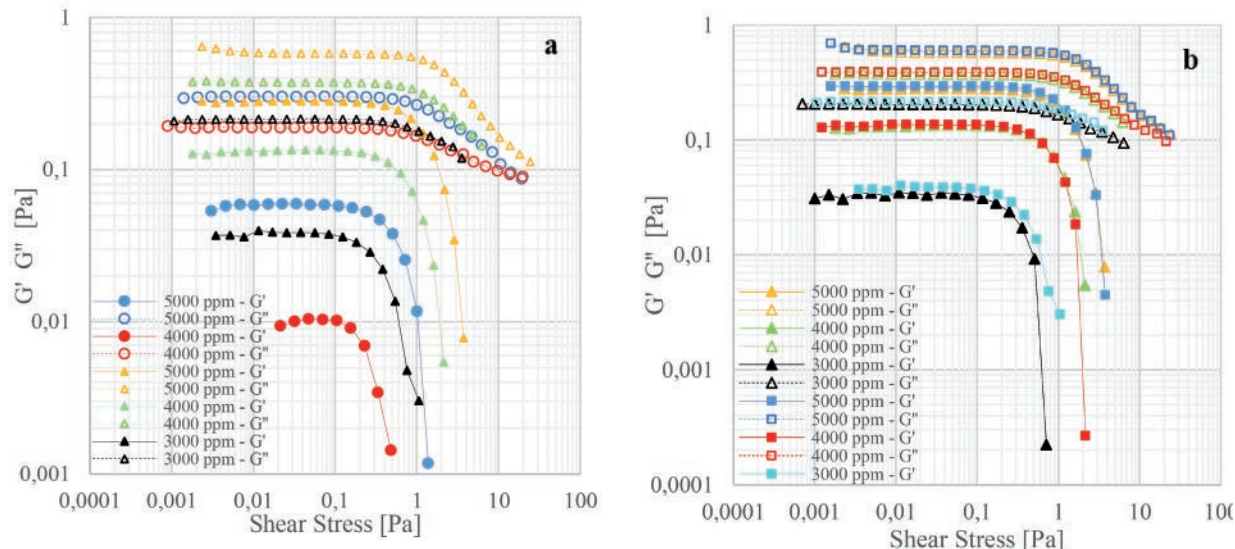


**Figure 8a, b.** AST results.  $G'$   $G''$  vs. Shear stress at 298.15 K. Where the **Circle** represents HPAM solutions with SB I, the **triangle** represent HPAM solutions with SB II and the **square** represents HPAM solutions with SB III.

Analyzing the Figure 8a, we can see a smaller LVR and a reduction of yield point when the solution includes divalent ions, due to higher ionic strength seems to reduce the strength of the intermolecular interactions (Perttamo., 2013). Similar performance has been reported for other authors (Silveira et al., 2016). For the HPAM solution with SB I (the highest divalent ions content) the LVR was present up to 4000 ppm. The other HPAM solution has LVR up to 3000 ppm.

In the figures, 8b is possible to see small changes in the viscoelastic behavior of the HPAM solutions with SB II and SB III. It due to the low difference in the  $Na^+$  content and the despite variation of the ionic strength. Comparing both, the HPAM solutions with SB III have better viscoelastic behavior than HPAM solutions with SB II.

Figures 9, 10 a,b evidence the temperature effect on the LVR behavior.

The LVR disappears for the HPAM solution with SB I at 323.15 K (Figure 9). In figures 10 a,b have identified the reduction of LVR when the temperature increase. For the HPAM solutions with SB II and SB III, the LVR is present up to 4000 ppm at 323.15 K.

The FST results for HPAM solutions with SB I and SB II show that the  $G'$  is more affected when the solution

includes divalent ions than the  $G''$  modulus (see Figure 11a). Thus, the measured value of elasticity decreased earlier at lower shear stress value for HPAM solution with SB I as compared to HPAM solution with SB II. Similar performance has been reported (Urbissinova et al., 2010).

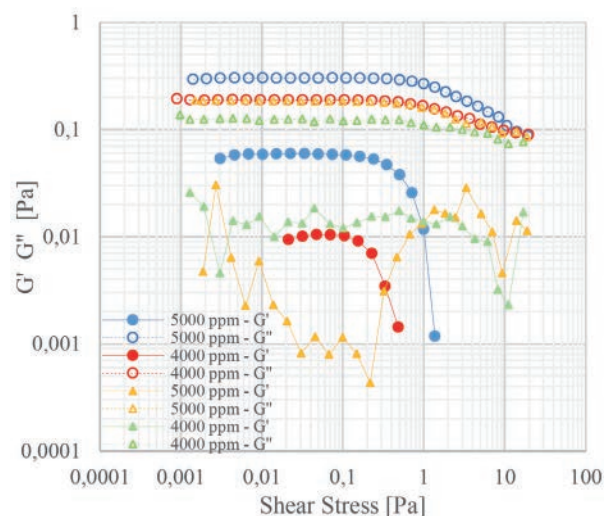


**Figure 9.** AST results.  $G'$   $G''$  vs. Shear Stress of HPAM solution with SB I. Where the **Circle** corresponds a temperature of 298.15 K, and the **triangle** corresponds a temperature of 323.15 K.

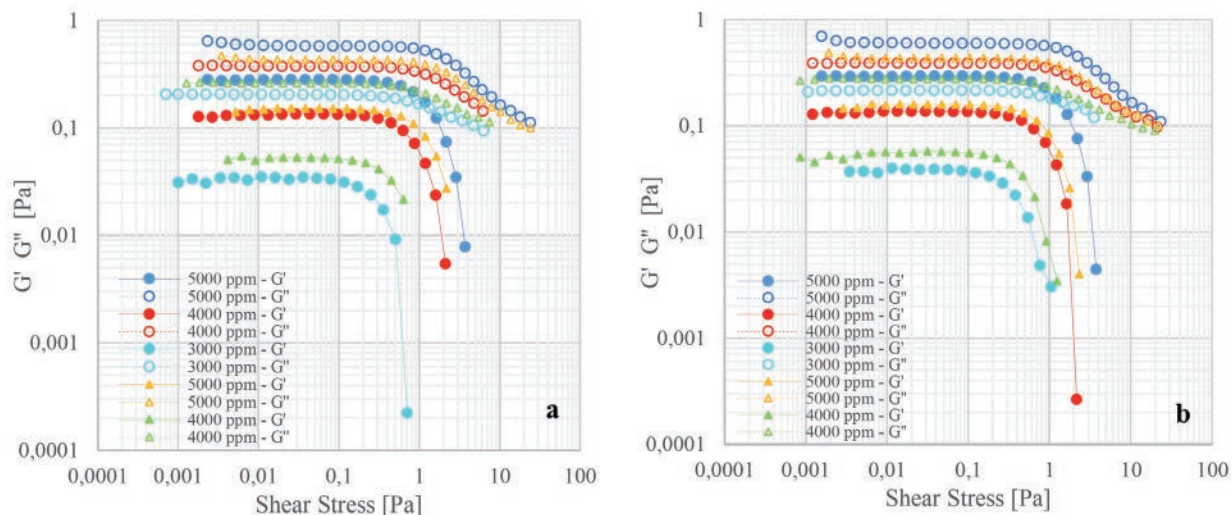


**Figure 10. a, b.** AST results.  $G'$   $G''$  vs. Shear Stress of HPAM solution with SB II and SB III, respectively. The Circles correspond to 298.15 K, while the triangles correspond to a temperature of 323.15 K

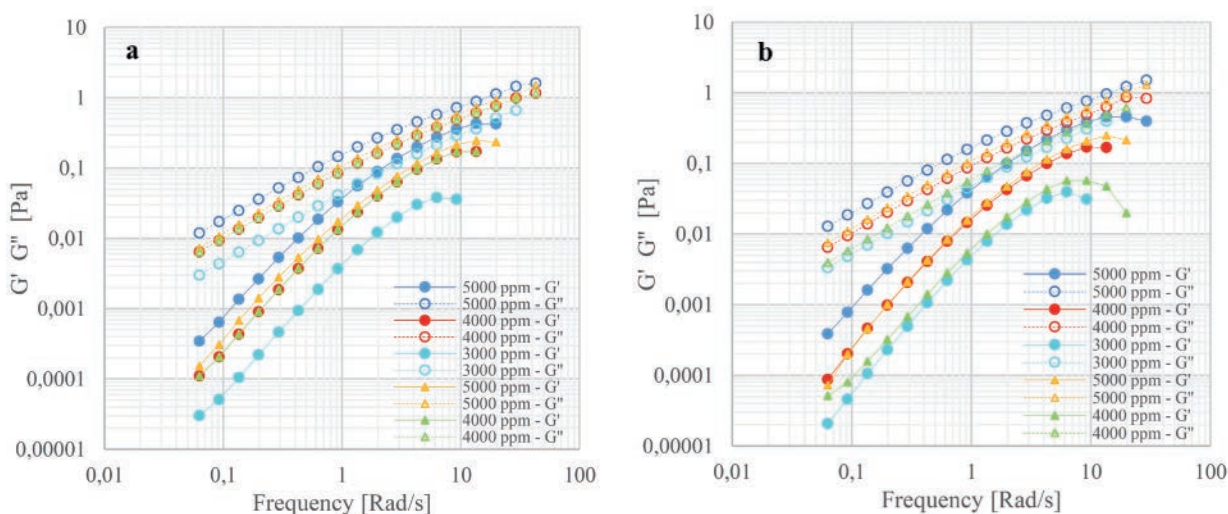


**Figure 11. a, b.** FST results.  $G'$   $G''$  vs. Shear Stress of HPAM solution with SB II and SB III, respectively. The Circles correspond to 298.15 K, while the triangles correspond to a temperature of 323.15 K.

## Conclusions

The polymeric solution with synthetic Brine III presented higher yield points values, a more extended Linear Viscoelastic Region, and higher viscosity values. Therefore, it shows the best rheological and viscoelastic performance.

The presence of divalent cations in the polymer solution reduced its viscosity more than the monovalent cations content. This observation agreed with the literature, and the effects are attributed to a more significant shielding effect of the former.

The overlap concentration is an inverse function of the shear rate for the tested polymeric solutions, i.e., the diluted regime range diminish while the semi-diluted raise when shear rate increases. On the other hand, the overlap concentration is a direct function of the temperature. As temperature increases, the dilute regime extends, and  $C^*$  is higher.

The increase in the polymer concentration raises the viscosity solution, while the rise in shear rate does the opposite.

Carreau-Yasuda model satisfactory adjusted the experimental data obtained for highly concentrated

polymer solutions. On the other hand, the use of Ostwald-de Waele Law was enough to fit the data for a solution with polymer concentration below 1000 ppm. Finally, the reduction of the linear viscoelastic region (LVR) was observed according to the decrease in polymer concentration into the solutions, increasing of temperature and the mono and divalent ions content. Under the tested conditions, the viscous modulus ( $G''$ ) was predominant for all solutions, and the elastic modulus ( $G'$ ) was more affected by the tested conditions. Can be expected that polymeric solutions less concentrated than 4000 ppm will have only a viscous influence on the oil recovery process.

This study contributes to the design of low molecular weight polymeric solutions. The results show that the polymer selected is not indicated for high salinity and high-temperature reservoirs.

### Acknowledgments

The authors wish to thank the Coordenação de Aperfeiçoamento de Pessoal de Nível Superior (CAPES) and the Department of Energy DE-FEM-UNICAMP for their support of this work.

### References

- Abidin, A.Z., Puspasari, T., Nugroho, W.A., 2012. Polymers for Enhanced Oil Recovery Technology. *Procedia Chem.* 4, 11–16. <https://doi.org/10.1016/j.proche.2012.06.002>.
- Al Hashmi, A.R., Al Maamari, R.S., Al Shabibi, I.S., Mansoor, A.M., Zaitoun, A., Al Sharji, H.H., 2013. Rheology and mechanical degradation of high-molecular-weight partially hydrolyzed polyacrylamide during flow through capillaries. *J. Pet. Sci. Eng.* 105, 100–106. <https://doi.org/10.1016/j.petrol.2013.03.021>.
- Barnes, Hutton & Walters, 1989. An Introduction to Rheology, *Journal of Non-Newtonian Fluid Mechanics*. [https://doi.org/10.1016/0377-0257\(89\)85015-3](https://doi.org/10.1016/0377-0257(89)85015-3).
- Bataweel, M.A. & Nasr-El-Din, H.A., 2012. Rheological Study for Surfactant-Polymer and Novel Alkali-Surfactant- Polymer Solutions 1–16. <https://doi.org/10.2118/150913-MS>.
- Cardenas, J.C., Lopéz, O.J. y Pinto, K.T., 2011. Estudio Reológico de los Fluidos Viscoelásticos Surfactantes Utilizados en Operaciones de Fracturamiento Hidráulico. *Rev. Fuentes El Reventón Energético* 9, 5–12.
- Castro-Garcia, R. H., Maya-Toro, G. A., Jimenez-Diaz, R., Quintero-Perez, H. I., Díaz-Guardia, V. M., Colmenares-Vargas, K. M., ... & Pérez-Romero, R. A. (2016). Polymer flooding to improve volumetric sweep efficiency in waterflooding processes. *CT&F-Ciencia, Tecnología y Futuro*, 6(3), 71-90.
- Díaz, R. J., Navarro, S. F. M., & Tavera, C. P. S. (2007). Modelo estadístico para la realización de analogías orientadas a procesos de recobro mejorado. *Fuentes: El reventón energético*, 5(1), 5.
- Ghosh, K. & Maiti, S.N., 1997. Melt Rheological Properties of Silver-Powder-Filled Polypropylene Composites. *Polym. Plast. Technol. Eng.* 36, 703–722. <https://doi.org/10.1080/03602559708000656>.
- Green, D.W. & Willhite, G.P., 1998. Enhanced Oil Recovery. Society of Petroleum Engineers Inc, Richardson, Texas.
- Huifen, X., Ye, J., Fanshun, K. & Junzheng, W., 2004. Effect of Elastic Behavior of HPAM Solutions on Displacement Efficiency Under Mixed Wettability Conditions. *Soc. Pet. Eng.* <https://doi.org/10.2118/90234-MS>.
- Jiang, H., Wu, W., Wang, D., Zeng, Y., Zhao, S. & Nie, J., 2008. The Effect of Elasticity on Displacement Efficiency in the Lab and Results of High Concentration Polymer Flooding in the Field. *Spe* 1–6. <https://doi.org/10.2118/115315-MS>.
- Lake, L.W., 1991. Enhanced Oil Recovery, Facsimile. ed, Enhanced Oil Recovery. Prentice-Hall, Englewood Cliffs. <https://doi.org/10.1016/B978-1-85617-855-6.00016-4>.
- Levitt, D.B. & Pope, G. a, 2008. Selection and Screening of Polymers for Enhanced-Oil Recovery. *Soc. Pet. Eng.* pp.1-18. SPE-113845. <https://doi.org/10.2118/113845-MS>.
- Littmann, W., 1988. Polymer Flooding, Developments in Petroleum Science. Elsevier B.V.
- Lopes, L.F., Silveira, B.M.O. & Moreno, R.B.Z.L.,

2014. Rheological Evaluation of HPAM fluids for EOR Applications. *Int. J. Eng. Technol. IJET-IJENS* 14, 35–41.
16. Maiti, S.N. & Mahapatro, P.K., 1988. Melt rheological properties of nickel powder filled polypropylene composites. *Polym. Compos.* 9, 291–296. <https://doi.org/10.1002/pc.750090408>.
17. Martín, C. A. G., García, R. E. P., Lizcano, J. C., & Buendía, H. L. (2014). Optimización de la metodología para el cálculo de porosidad a través de saturación de fluidos. *Fuentes: El reventón energético*, 12(2), 7.
18. Martín, C. A. G., & Páez, E. G. M. (2017). Efeito da salinidade na tensão interfacial do sistema óleo/água em condições isobáricas e incremento gradual da temperatura. *Fuentes: El reventón energético*, 15(2), 117-124.
19. Melo, M.A., de Holleben, C., da Silva, I.P.G., de Barros Correia, A., da Silva, G.A., Rosa, A.J., Lins, A.G. & de Lima, J.C., 2005. Evaluation of Polymer Injection Projects in Brazil. *Lat. Am. Caribb. Pet. Eng. Conf.* 17. SPE-94898. <https://doi.org/10.2523/94898-MS>.
20. Melo, M.A. De, Silva, I.P.G., Godoy, G.M.R. De, Sanmartim, A.N., Petrobras, S.A., 2002. Polymer Injection Projects in Brazil: Dimensioning, Field Application and Evaluation. *SPE/DOE Thirteen. Symp. Improv. Oil Recover.* 11. <https://doi.org/10.2118/75194-MS>.
21. Melo, M. De, Lucas, E., 2008. Characterization and Selection of Polymers for Future Research on Enhanced Oil Recovery. *Chem. Chem. Technol.* 2, 295–303.
22. Molano, A. M. J., Navarro, S. F. M., & Díaz, R. J. (2014). Metodología para el diseño de baches en un proceso de inyección de polímeros para recobro mejorado, considerando fenómenos de interacción roca/fluidos. *Fuentes: El reventón energético*, 12(2), 6.
23. Muller, G., 1981. Thermal stability of high-molecular-weight polyacrylamide aqueous solutions. *Polym. Bull.* 5, 31–37. <https://doi.org/10.1007/BF00255084>.
24. Needham, R.B., Co, P.P. & Doe, P.H., 1987. Polymer Flooding Review. *J. Pet. Technol.* 1503–1507. <https://doi.org/10.2118/17140-PA>
25. Ordoñez, J., & Fajardo, R. (2015). Estudio inicial de geo-polímeros a partir de arcillas. *Revista Fuentes*, 13(2).
26. Perttamo, E.K., 2013. Characterization of Associating Polymer (AP) Solutions. *Dep. Phys. Technol. Cent. Integr. Pet. Res. Master*, 145.
27. Reichenbach-Klinke, R., Langlotz, B., Wenzke, B., Spindler, C., Brodt, G., 2011. Hydrophobic Associative Copolymer with Favourable Properties for the Application in Polymer Flooding. *SPE Int. Symp. Oilf. Chem.* 1–11. <https://doi.org/10.2118/141107-MS>.
28. Samanta, A., Bera, A., Ojha, K. & Mandal, A., 2010. Effects of alkali, salts, and surfactant on rheological behavior of partially hydrolyzed polyacrylamide solutions. *J. Chem. Eng. Data* 55, 4315–4322. <https://doi.org/10.1021/je100458a>.
29. Sheng, J.J., 2013. *Enhanced Oil Recovery Field Case Studies*. Elsevier.
30. Sheng, J.J., 2011. *Modern Chemical Enhanced Oil Recovery, Modern Chemical Enhanced Oil Recovery*. Elsevier. <https://doi.org/10.1016/B978-1-85617-745-0.00001-2>.
31. Silveira, B.M.O., Lopes, L.F. & Moreno, R.B.Z.L., 2016. Rheological Approach of HPAM Solutions under Harsh Conditions for EOR Applications 1-8.
32. Sorbie, K.S., 2013. *Polymer-improved oil recovery*. Springer Science & Business Media., New York. <https://doi.org/10.1007/978-94-011-3044-8>.
33. Urbissinova, T.S., Trivedi, J.J. & Kuru, E., 2010. Effect of elasticity during viscoelastic polymer flooding: A possible mechanism of increasing the sweep efficiency. *J. Can. Pet. Technol.* 49, 49–56. <https://doi.org/10.2118/133471-PA>.
34. Wang, D., Cheng, J., Xia, H., Li, Q., Shi, J., LTD, D.O.I.L.C.O., 2001. Viscous-Elastic Fluids Can Mobilize Oil Remaining After Water-Flood By Force Parallel To the Oil-Water Interface. *Spe*

Asia Pacific Impr. Oil Recover. Conf. [Apiore 2001] (Kuala Lumpur, Malaysia, 10/8-9/2001) Proc. <https://doi.org/10.2118/72123-MS>.

29. Wang, D., Han, P., Shao, Z., Hou, W., Seright, R.S., 2008. Sweep-Improvement Options for the Daqing Oil Field. SPE Reserv. Eval. Eng. 22–26. <https://doi.org/10.2118/99441-PA>.

30. Wang, D., Wang, G., Wu, W., Xia, H. & Yin, H., 2007. The Influence of Viscoelasticity on Displacement Efficiency - From Micro- To Macroscale. SPE Annu. technical Conf. <https://doi.org/10.2118/109016-MS>.

31. Yasuda, K., Armstrong, R.C. & Cohen, R.E., 1981. Shear flow properties of concentrated solutions of linear and star branched polystyrenes. Rheol. Acta 20, 163-178. <https://doi.org/10.1007/BF01513059>.

32. Zhou, G., Willett, J.L. & Carriere, C.J., 2000. Temperature dependence of the viscosity of highly starch-filled poly(hydroxy ester ether) biodegradable composites. Rheol. Acta 39, 601–606. <https://doi.org/10.1007/s003970000096>.

33. Zhu, D., Wei, L., Wang, B. & Feng, Y., 2014. Aqueous hybrids of silica nanoparticles and hydrophobically associating hydrolyzed polyacrylamide used for EOR in high-temperature and high-salinity reservoirs. Energies 7, 3858–3871. <https://doi.org/10.3390/en7063858>.

### Appendix A

**Table A 1.** Fit parameters used for Carreau-Yasuda model on Polymer Solution with Synthetic Brine I.

Polymer concentration	$\eta_0$		$\eta_\infty$		$\lambda$		$\eta$		$a$		$R^2$	
	ppm	298.15 K	323.15 K	298.15 K	323.15 K	298.15 K	323.15 K	298.15 K	323.15 K	298.15 K	323.15 K	298.15 K
5000	0.0624	0.0323	0.00093	0.0006	0.1521	0.0804	0.6660	0.6918	2	2	0.9990	0.9984
4000	0.0349	0.0178	0.00093	0.0006	0.1153	0.0481	0.7122	0.7237	2	2	0.9990	0.9989
3000	0.0174	0.0095	0.00093	0.0006	0.0745	0.0412	0.7819	0.8046	2	2	0.9988	0.9873
2000	0.0087	0.0083	0.00093	0.0006	0.0873	1139	0.8621	0.9299	2	2	0.9469	0.7600
1500	0.0058	-	0.00093	0.0006	0.2430	-	0.9306	-	2	2	0.7786	-

**Table A 2.** Fit parameters used for Ostwald-de Waele Law on Polymer Solution with Synthetic Brine I.

Polymer concentration	$K$		$\eta$		$R^2$	
ppm	298.15 K	323.15 K	298.15 K	323.15 K	298.15 K	323.15 K
5000	0.1264	0.0697	0.6556	0.6950	0.9999	0.9988
4000	0.0677	0.0431	0.7117	0.7224	0.9995	0.9996
3000	0.0300	0.0182	0.7851	0.8013	0.9995	0.9999
2000	0.0119	0.0056	0.8661	0.9263	0.9994	0.9995
1500	0.0063	0.0034	0.9303	0.9705	0.9992	0.9997
1000	0.0037	0.0021	0.9584	0.9743	0.9996	0.9997
800	0.0031	0.0018	0.9605	0.9755	0.9998	0.9998
600	0.0024	0.0014	0.9664	0.9916	1.0000	0.9998
400	0.0018	0.0011	0.9837	0.9800	1.0000	0.9998
300	0.0016	0.0009	0.9862	1.0000	0.9999	1.0000
200	0.0013	0.0008	0.9911	1.0000	0.9990	0.9999
100	0.0013	0.0007	0.9749	1.0000	0.9999	0.9998

**Table A 3.** Fit parameters used for Carreau-Yasuda model on Polymer Solution with Synthetic Brine II.

Polymer concentration	$\eta_0$		$\eta_\infty$		$\lambda$		$n$		$a$		$R^2$	
	298.15 K	323.15 K	298.15 K	323.15 K	298.15 K	323.15 K	298.15 K	323.15 K	298.15 K	323.15 K	298.15 K	323.15 K
ppm												
5000	0.1943	0.1077	0.00093	0.0006	0.5215	0.2741	0.6151	0.6252	2	2	0.9989	0.9990
4000	0.1042	0.0620	0.00093	0.0006	0.3408	0.1893	0.6445	0.6511	2	2	0.9988	0.9980
3000	0.0485	0.0270	0.00093	0.0006	0.2117	0.0925	0.6871	0.6887	2	2	0.9985	0.9970
2000	0.0200	0.0118	0.00093	0.0006	0.1192	0.0658	0.7537	0.7653	2	2	0.9985	0.9960
1500	0.0120	0.0069	0.00093	0.0006	0.1308	0.0496	0.8136	0.8472	2	2	0.9888	0.8430
1000	0.0066	-	0.00093	0.0006	0.1941	-	0.8918	-	2	2	0.8823	-

**Table A 4.** Fit parameters used for Ostwald-de Waele Law on Polymer Solution with Synthetic Brine II.

Polymer concentration	$K$		$\eta$		$R^2$	
	298.15 K	323.15 K	298.15 K	323.15 K	298.15 K	323.15 K
ppm						
5000	0.2465	0.1781	0.6131	0.6232	0.9969	0.9977
4000	0.1487	0.1136	0.6475	0.6541	0.9979	0.9989
3000	0.0793	0.0586	0.6885	0.6886	0.9990	0.9993
2000	0.0338	0.0232	0.7567	0.7618	0.9978	0.9994
1500	0.0175	0.0122	0.8157	0.8455	0.9988	0.9993
1000	0.0076	0.0041	0.8937	0.9549	0.9991	0.9992
800	0.0052	0.0030	0.9357	0.9671	0.9996	0.9996
600	0.0040	0.0024	0.9384	0.9594	0.9997	0.9998
400	0.0027	0.0017	0.9513	0.9705	0.9999	0.9999
300	0.0022	0.0013	0.9611	0.9848	1.0000	1.0000
200	0.0017	0.0010	0.9832	0.9923	1.0000	1.0000
100	0.0013	0.0009	0.9901	0.9888	0.9999	0.9993

**Table A 5.** Fit parameters used for Carreau-Yasuda model on Polymer Solution with Synthetic Brine III.

Polymer concentration	$\eta_0$		$\eta_\infty$		$\lambda$		$\eta$		$a$		$R^2$	
	298.15 K	323.15 K	298.15 K	323.15 K	298.15 K	323.15 K	298.15 K	323.15 K	298.15 K	323.15 K	298.15 K	323.15 K
ppm												
5000	0.2165	0.1185	0.00093	0.0006	0.5757	0.2733	0.6122	0.6153	2	2	0.9991	0.9989
4000	0.1126	0.0644	0.00093	0.0006	0.4537	0.1848	0.6575	0.6430	2	2	0.9969	0.9988
3000	0.0552	0.0321	0.00093	0.0006	0.3128	0.1083	0.6883	0.6753	2	2	0.9949	0.9990
2000	0.0225	0.0137	0.00093	0.0006	0.1364	0.0755	0.7339	0.7710	2	2	0.9987	0.9980
1500	0.0416	0.0089	0.00093	0.0006	1050	0.2445	0.8431	0.8341	2	2	0.9234	0.9356
1000	0.0317	-	0.00093	-	3144	-	0.8463	-	2	-	0.9368	-

**Table A 6.** Fit parameters used for Ostwald-de Waele Law on Polymer Solution with Synthetic Brine III.

Polymer concentration ppm	<i>K</i>		$\eta$		<i>R</i> <sup>2</sup>	
	298.15 K	323.15 K	298.15 K	323.15 K	298.15 K	323.15 K
5000	0.2808	0.1858	0.6138	0.6178	0.9960	0.9957
4000	0.1626	0.1106	0.6559	0.6428	0.9994	0.9971
3000	0.0902	0.0652	0.6820	0.6752	0.9996	0.9987
2000	0.0419	0.0245	0.7357	0.7706	0.9983	0.9979
1500	0.0169	0.0119	0.8420	0.8325	0.9984	0.9999
1000	0.0097	0.0048	0.8450	0.9366	0.9998	0.9984
800	0.0081	0.0036	0.8544	0.9447	1.0000	0.9993
600	0.0045	0.0026	0.9242	0.9589	0.9994	0.9990
400	0.0030	0.0017	0.9436	0.9768	1.0000	1.0000
300	0.0022	0.0014	0.9693	0.9727	0.9999	1.0000
200	0.0019	0.0011	0.9613	0.9939	0.9990	1.0000
100	0.0013	0.0008	0.9916	1.0000	0.9999	0.9990

## Appendix B

**Table B 1.** Fit parameters used for Arrhenius equation on Polymer Solutions.

Concentration (ppm)	Synthetic Brine I		Synthetic Brine II		Synthetic Brine III	
	$\Delta E_{\eta}$ (kJ/mol)	A (Pa*s)	$\Delta E_{\eta}$ (kJ/mol)	A (Pa*s)	$\Delta E_{\eta}$ (kJ/mol)	A (Pa*s)
5000	18.374	3.196E-05	12.630	7.115E-04	12.068	9.572E-04
4000	18.846	1.570E-05	12.055	5.646E-04	11.714	6.632E-04
3000	18.068	1.141E-05	14.645	1.066E-04	12.038	3.254E-04
2000	19.628	3.110E-06	15.132	4.083E-05	13.820	7.604E-05
1500	18.474	3.276E-06	14.989	2.672E-05	13.843	4.627E-05
1000	17.407	3.141E-06	15.097	1.436E-05	12.798	3.743E-05
800	17.333	2.616E-06	15.065	1.089E-05	14.823	1.336E-05
600	16.393	3.042E-06	14.873	8.842E-06	14.711	1.020E-05
400	15.043	3.981E-06	15.266	5.257E-06	16.663	3.211E-06
300	16.973	1.635E-06	15.645	3.708E-06	13.588	8.495E-06
200	14.713	3.392E-06	15.073	3.679E-06	13.610	6.935E-06
100	16.064	1.814E-06	13.019	6.498E-06	13.172	6.212E-06

## Appendix C

**Table C 1.** Overlapping concentration on Polymer solution with Synthetic Brine I+.

Shear Rate (s <sup>-1</sup> ) @ Temperature 298.15 K	Dashed Lines			Continuous Lines			<i>C</i> * (ppm)
	a	b	<i>R</i> <sup>2</sup>	a	b	<i>R</i> <sup>2</sup>	
7.8	0.2120	0.3585	0.9010	7E-06	1.8511	0.9910	992.85
143.8	0.2893	0.2945	0.9042	0.0002	1.3565	0.9958	945.84
Shear Rate (s <sup>-1</sup> ) @ Temperature 323.15 K	Dashed Lines			Continuous Lines			<i>C</i> * (ppm)
	a	b	<i>R</i> <sup>2</sup>	a	b	<i>R</i> <sup>2</sup>	
7.8	0.1953	0.2760	0.9236	9E-07	2.0219	0.9953	1139.11

**Table C 2.** Overlapping concentration on Polymer solution with Synthetic Brine II+.

Shear Rate (s <sup>-1</sup> ) @ Temperature 298.15 K	Dashed Lines			Continuous Lines			C* (ppm)
	a	b	R <sup>2</sup>	a	b	R <sup>2</sup>	
7.8	0.1235	0.4933	0.9796	7E-06	1.9451	0.9979	845.78
143.8	0.2073	0.3827	0.9783	0.0006	1.2808	0.9975	670.60
Shear Rate (s <sup>-1</sup> ) @ Temperature 323.15 K	Dashed Lines			Continuous Lines			C* (ppm)
	a	b	R <sup>2</sup>	a	b	R <sup>2</sup>	
7.8	0.1050	0.4391	0.9954	1E-06	2.1279	0.9976	940.22

**Table C 3.** Overlapping concentration on Polymer solution with Synthetic Brine III+.

Shear Rate (s <sup>-1</sup> ) @ Temperature 298.15 K	Dashed Lines			Continuous Lines			C* (ppm)
	a	b	R <sup>2</sup>	a	b	R <sup>2</sup>	
7.8	0.1131	0.5168	0.9675	2E-05	1.8244	0.9961	740.82
143.8	0.2186	0.377	0.9969	0.0009	1.2218	0.9986	666.25
Shear Rate (s <sup>-1</sup> ) @ Temperature 323.15 K	Dashed Lines			Continuous Lines			C* (ppm)
	a	b	R <sup>2</sup>	a	b	R <sup>2</sup>	
7.8	0.1012	0.455	0.9919	4E-06	1.9689	0.9981	809.96

\*Adjusted by potential trend line:  $\eta = a \cdot c^b$ , where  $\eta$  is the viscosity (mPa\*s),  $c$  is the concentration (ppm),  $a$  and  $b$  are constants.

**Recepción:** 17 de enero de 2018

**Aceptación:** 25 de mayo de 2018